ACS APPLIED MATERIALS & INTERFACES

Research Article

www.acsami.org

Redox-Responsive Polycation-Functionalized Cotton Cellulose Nanocrystals for Effective Cancer Treatment

Hao Hu,[†,‡,§,△] Wei Yuan,[∥,△] Fu-Sheng Liu,[⊥] Gang Cheng,[#] Fu-Jian Xu,*[,†,‡,§] and Jie Ma*[,∥]

[†]State Key Laboratory of Chemical Resource Engineering, College of Materials Science & Engineering, Beijing University of Chemical Technology, Beijing 100029, China

[‡]Key Laboratory of Carbon Fiber and Functional Polymers (Beijing University of Chemical Technology), Ministry of Education, Beijing 100029, China

[§]Beijing Laboratory of Biomedical Materials, Beijing University of Chemical Technology, Beijing 100029, China

[∥]State Key Laboratory of Molecular Oncology, Cancer Hospital, Chinese Academy of Medical Sciences, Beijing 100021, China

[⊥]Brain Tumor Research Center, Beijing Neurosurgical Institute, Beijing Tiantan Hospital affiliated with Capital Medical University, Beijing 100050, China

[#]Department of Chemical and Biomolecular Engineering, University of Akron, Akron, Ohio 44325, United States

Supporting Information

ABSTRACT: Carbon nanotubes have excellent penetrability and encapsulation efficiency in the fields of drug and gene delivery. Because of their excellent physicochemical properties, biocompatible rodlike cellulose nanocrystals (CNCs) were reportedly expected to replace carbon nanotubes. In this work, CNCs from natural cotton wool were functionalized with disulfide bond-linked poly(2-(dimethylamino)ethyl methacrylate) (PDMAEMA) brushes for effective biomedical applications. A range of CNC-*graft*-PDMAEMA vectors (termed as CNC-SS-PDs) with various molecular weights of PDMAEMA were synthesized. Under reducible conditions, PDMAEMA chains can be easily cleaved from CNCs. The gene condensation ability, reduction sensitivity, cytotoxicity, gene transfection, and in vivo antitumor activities of CNC-SS-PDs were investigated in detail. The CNC-SS-PDs exhibited good transfection efficiencies and low cytotoxicities. The needlelike shape of CNCs had an important effect on enhancing transfection efficiency. The antitumor effect of CNC-SS-PDs was evaluated by a suicide gene/prodrug system (cytosine deaminase/5-fluorocytosine, CD/5-FC) in vitro and in vivo. This research demonstrates that the functionalization of CNCs with redox-responsive polycations is an effective method for developing novel gene delivery systems.

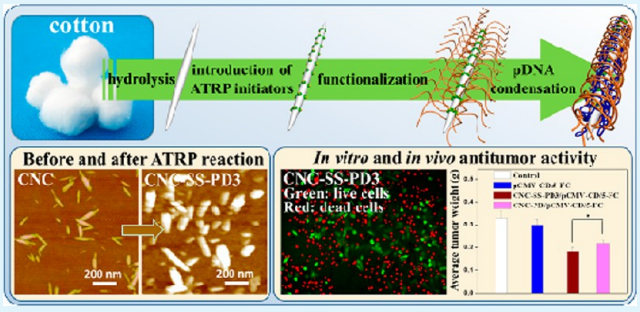

KEYWORDS: *cellulose, bioreducible, ATRP, PDMAEMA, gene transfection, antitumor*

1. INTRODUCTION

Traditional treatments of cancer, including excision, chemotherapy, and radiotherapy, are limited by unsatisfactory effects and safety concerns. Gene therapy is an encouraging therapeutic method for severe diseases, such as cancer, AIDS, and cardiovascular diseases.[1−3] The major challenge in gene therapy is the lack of ideal gene vectors that possess high transfection efficiency but low cytotoxicity.[4,5] Traditional viral vectors show high transfection efficiency but also significant toxicity and immunogenicity.[6] Nonviral vectors have increasingly attracted much attention. Cationic vectors, such as polyethylenimine (PEI) derivatives,[7,8] chitosan,[9] poly(2-(dimethylamino)ethyl methacrylate) (PDMAEMA),[10,11] and poly(L-lysine),[12] have been widely investigated due to their electropositivity and low immunogenicity. However, the balance of transfection and toxicity requires further refinement.

Numerous nanoparticle (NP)-based drug carriers exhibit great potential and applied values due to their stability, specific morphology, good biocompatibility, and ease of surface modification.[13] Compared to spherical nanoparticles, rodlike particles are internalized faster.[14] Our recent work illustrates that rodlike NPs have a significant impact on gene transfection.[4] It is well-known that carbon nanotubes have excellent penetrability and encapsulation efficiency in the fields of drug and gene delivery.[15] Recently, it was reported that, due to their excellent physicochemical properties, rodlike cellulose nanocrystals (CNCs) were expected to replace carbon nanotubes.[16] CNCs with typical sizes of <300 nm in length and 10 nm in diameter could be readily obtained via hydrolysis of

Received: March 19, 2015
Accepted: April 7, 2015
Published: April 7, 2015

DOI: 10.1021/acsami.5b02432
ACS Appl. Mater. Interfaces 2015, 7, 8942−8951

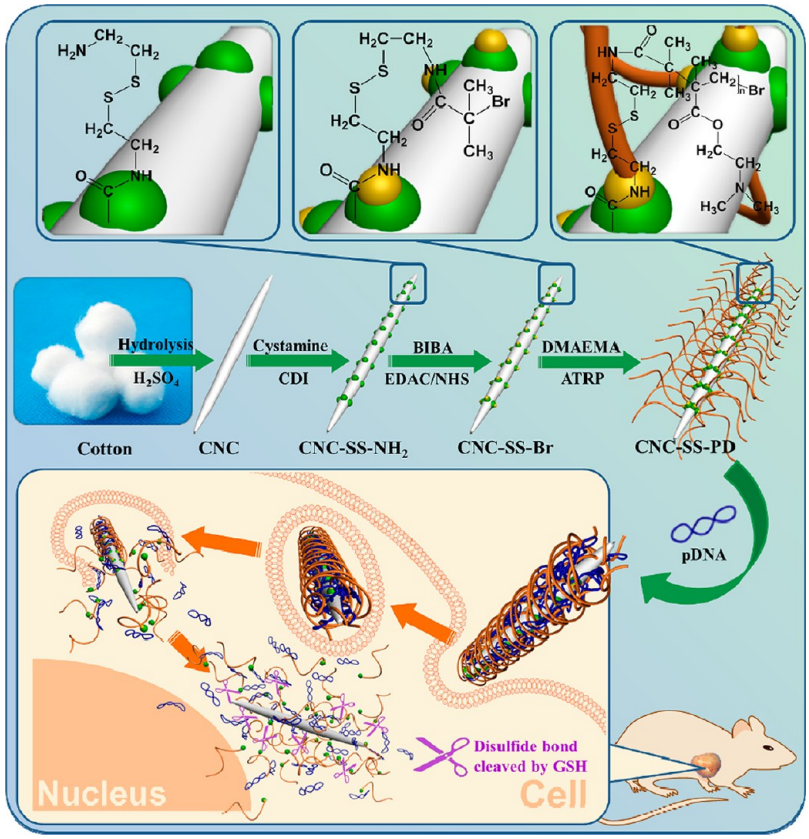

Figure 1. Schematic diagram illustrating the preparation of CNC-*graft*-PDMAEMA (CNC-SS-PD) via ATRP and the resultant gene delivery process.

celluloses.[17,18] Relative to carbon nanotubes, cellulose is a natural polysaccharide with outstanding properties, such as renewability, easy preparation, biodegradability, and no cytotoxicity.[19−21] In addition, CNCs have large surface areas,[22] and the numerous hydroxyls on the surface of CNCs can be used for surface modification.[18] On the basis of these properties, CNCs are potential candidates for drug and gene delivery. It was reported that PDMAEMA can effectively condense DNA into nanoparticles to facilitate cellular internalization for gene delivery.[10,23] Thus, it could be possible to design new CNC-based gene carriers if CNCs are wrapped with dense PDMAEMA brushes.

Disulfide bonds can be reduced by reducing reagents, such as glutathione (GSH), in tumor tissues.[24−26] Redox-responsive cationic vectors containing disulfide bonds show better performance of gene delivery.[27−29] Herein, a flexible method was proposed to functionalize CNCs with disulfide bond-linked PDMAEMA side chains for effective biomedical applications. Atom transfer radical polymerization (ATRP) is a controlled polymerization for fine synthesis.[30] In this work, ATRP initiation sites with disulfide bonds were first immobilized onto CNC surfaces (Figure 1). Then, a series of redox-responsive nanocomposites (CNC-SS-PDs) composed of CNCs and biocleavable PDMAEMA brushes were prepared by ATRP. The gene condensation ability, reduction sensitivity, cytotoxicity, gene transfection, and cellular uptake of CNC-SS-PDs were investigated in detail. The in vitro and in vivo antitumor effects of the gene vectors were evaluated by the suicide gene/prodrug system (cytosine deaminase/5-fluorocytosine (CD/5-FC)[31]).

2. EXPERIMENTAL SECTION

2.1. Materials. Branched polyethylenimine (PEI, $M_w \sim 25000$ Da), cystamine dihydrochloride (>98%), 1,1′-carbonyldiimidazole (CDI, 97%), α-bromoisobutyric acid (BIBA, 98%), *N*-hydroxysuccinimide (NHS, 98%), 1-ethyl-3-(3-(dimethylamino)propyl)carbodiimide hydrochloride (EDAC, 98%), 2,2′-byridine (Bpy, 99%), copper(I) bromide (CuBr, 99%), 2-(dimethylamino)ethyl methacrylate (DMAEMA, >98%), fluorescein diacetate (FDA, >98%), propidium iodinate (PI, >98%), D-mannitol (>99%), 3-(4,5-dimethylthiazol-2yl)-2,5-diphenyltetrazolium bromide (MTT), and 5-fluorocytosine were obtained from Sigma-Aldrich Chemical (St. Louis, MO, USA). Inhibitors in DMAEMA were removed by an inhibitor-removal column (Sigma-Aldrich). COS7 and HepG2 cells were obtained from the American Type Culture Collection (ATCC, Rockville, MD, USA). Female Balb/c-nu mice were obtained from the Institute of Laboratory Animal Sciences (ILAS). The plasmid DNAs (pDNA) used, including pRL-CMV encoding Renilla luciferase, pEGFP-N1 encoding enhanced green fluorescent protein (EGFP), and pAdTrack-CMV-CD (pCMV-CD) encoding *Escherichia coli* cytosine deaminase (ECD), were amplified and purified as described earlier.[10]

2.2. Preparation of Cellulose Nanocrystals (CNCs). CNCs were hydrolyzed by sulfuric acid as described by Morandi et al.[20] Briefly, cotton wool was dispersed in sulfuric acid (64 wt %) and incubated at 45 °C for 35 min. The resulting precipitation was washed three times by centrifugation at 10000 rpm and 10 °C for 20 min. Dialysis was performed for 1 week. The suspension was then filtered via membranes with pore sizes of 0.2 μm to remove residual aggregates prior to lyophilization.

2.3. Preparation of Disulfide Bond-Containing ATRP Initiation Sites. The ATRP initiation sites were introduced onto CNC surfaces through two steps (Figure 1). The −OH groups on CNCs were activated to react with cystamine and produce the disulfide bond-containing CNCs (CNC-SS-NH_2) as described previously.[32] Briefly, CDI (0.5 g in 3 mL of DMSO) was added to a

DOI: 10.1021/acsami.5b02432
ACS Appl. Mater. Interfaces 2015, 7, 8942−8951

CNC suspension (2.5 g in 25 mL of DMSO), and the resultant mixture was stirred for 24 h. Then, cystamine dihydrochloride (5 g in 10 mL of DMSO) and triethylamine (TEA, 3 mL) were added to the CDI-activated CNC suspension. The mixture was reacted in nitrogen atmosphere at 25 °C for another 24 h. The final reaction mixture was centrifuged three times with a water/MeOH mixture (50:50, v/v), before CNC-SS-NH_2 was redispersed by sonication and dialyzed (MWCO 3500). The final CNC-SS-NH_2 was freeze-dried. For the control group (CNC-NH_2) without disulfide bonds, cystamine dihydrochloride was replaced with ethylenediamine. Other steps are the same as described above.

CNC-SS-NH_2 was then reacted with BIBA to prepare the bromoisobutylryl-terminated CNCs (CNC-SS-Br).[32] Briefly, BIBA (1.00 g), EDAC (1.37 g), NHS (0.83 g), and TEA (1.5 mL) were added to 10 mL of DMSO, and the solution was stirred at 37 °C for 4 h. Then, CNC-SS-NH_2 (1.0 g) in 10 mL of DMSO and TEA (1 mL) was added to the solution. The reaction mixture was reacted in a nitrogen atmosphere at 37 °C for 2 days. The final reaction mixture was centrifuged three times with water-MeOH mixture (50/50, v/v) and dialyzed (MWCO 3500). The end-product was freeze-dried to obtain CNC-SS-Br. The corresponding control CNC-Br was prepared by replacing CNC-SS-NH_2 with CNC-NH_2 under similar reaction conditions as described above.

2.4. Synthesis of Biocleavable Carriers via ATRP. CNC-SS-Br (50 mg) was grafted with PDMAEMA via ATRP at a molar feed ratio of 50:2.5:1 ([DMAEMA, 1 mL]/[Bpy]/[CuBr]) to produce CNC-*graft*-PDMAEMA vectors (termed as CNC-SS-PD) (Figure 1). The reaction was performed under typical ATRP conditions as described previously.[10,33] CNC-SS-Br, Bpy, and DMAEMA were added to 5 mL of a methanol/water mixture (2:3, v/v). Then, CuBr was added in a nitrogen atmosphere. The polymerization was performed from 2 to 30 min at room temperature. The resultant reaction mixture was dialyzed (MWCO 3500) prior to lyophilization. For the control CNC-PD without disulfide bonds (Table 1), the experimental conditions were controlled similar to those of CNC-SS-PD to ensure comparable physiochemical characteristics (except reducibility) were obtained. The ATRP time of CNC-PD was 10 min, and all other steps were the same as described above.

Table 1. Characterization of Functionalized CNCs

sample	reaction time (min)	M_n (g/mol)[c]	PDI[c]
CNC-SS-PD1[a]	2	5.1×10^3	1.23
CNC-SS-PD2[a]	5	5.9×10^3	1.22
CNC-SS-PD3[a]	10	6.6×10^3	1.26
CNC-SS-PD4[a]	20	7.4×10^3	1.23
CNC-SS-PD5[a]	30	8.0×10^3	1.31
CNC-PD[b]	10	6.2×10^3	1.25

[a]Incubated with DTT for 24 h to cleave PDMAEMA side chains. The supernatant for GPC measurements was collected by centrifugation. [b]Hydrolyzed with H_2SO_4 for 3 h at 45 °C to cleave PDMAEMA side chains. [c]Determined from GPC. Polydispersity index (PDI) = weight, or M_w/M_n

2.5. Characterization of Materials. The CNC-SS-PDs were characterized by gel permeation chromatography (GPC, YL9100), atomic force microscopy (AFM, Veeco, Santa Barbara, CA, USA), X-ray photoelectron spectroscopy (XPS, Kratos AXIS HSi spectrometer), and Fourier transform infrared (FTIR, ThermoScientific) spectroscopy. The detailed procedures have been described in our earlier work.[4,10]

2.6. Characterization of CNC-SS-PD/pDNA Complexes. CNC-SS-PD-to-DNA (or CNC-PD-to-DNA) ratios were expressed as the molar ratios of nitrogen (N) in PDMAEMA to phosphate (P) in pDNA (or as N/P ratios) as described previously.[10] The ability of CNC-SS-PD (or CNC-PD) to bind pDNA, the reduction-triggered degradation of CNC-SS-PD/pDNA complexes, and the heparin-induced release of pDNA were assayed by agarose gel electrophoresis as described previously.[10,34,35] Particle size and ζ-potential of CNC-SS-PD/pDNA complexes were tested by dynamic light scattering (Nano-ZS90).[10,33] The morphologies of CNC-SS-PD/pDNA complexes were observed intuitively by AFM.

2.7. In Vitro Cytotoxicity Assay. The cytotoxicity of cationic complexes was analyzed by MTT assays in COS7 and HepG2 cells. Briefly, cells were seeded in 96-well plates for 24 h. The culture medium was replaced with fresh medium containing polycation/pDNA complexes at various N/P ratios. After 24 h, MTT reagent was added to each well. Detailed procedures have been described previously.[10,32]

2.8. Cellular Uptake. HepG2 cells were used, and pRL-CMV was labeled with YOYO-1 (green molecular probe) as described previously.[10,36] Cells were seeded onto 6-well plates for 24 h, and then the complexes at N/P = 15 were added to each well in succession. The plate was incubated for another 4 h, and then the cultured HepG2 cells were detached and resuspended in 1.5 mL of PBS. The fluorescence intensity of positive HepG2 cells was assessed by a flow cytometer (BD LSR II, BD, Franklin Lakes, NJ, USA). For the fluorescence imaging, the cultured cells were stained with 4′,6′-diamidino-2-phenylindole (DAPI, 150 ng/mL in PBS) for 10 min and washed with methanol. The fluorescent images were taken on a Leica DMI3000B fluorescence microscope.

2.9. In Vitro Transfection Assay. Transfection was first performed in COS7 and HepG2 cells using plasmid pRL-CMV. Briefly, cells were seeded on 24-well plates and incubated for 24 h. Complexes (20 μL/well containing 1.0 μg of pRL-CMV) at various N/P ratios were added. After 4 h, the medium was replaced with fresh medium. After an additional 20 h, the cultured cells were washed and lysed for transfection assays. Moreover, the transfection efficiency of complexes was also analyzed at their optimal N/P ratios with pEGFP in HepG2 cells. The EGFP-positive cells were imaged by a Leica DMI3000B fluorescence microscope and counted by a flow cytometer (BD LSR II, BD, Franklin Lakes, NJ).[37] Detailed procedures have been described previously.[10,32]

2.10. In Vitro Antitumor Activity. HepG2 cells were seeded in 96-well plates (1×10^4 cells/well). After 24 h of incubation, the medium was replaced with fresh medium containing CNC-SS-PD/pCMV-CD complexes (suicide gene, 0.3 μg/well, N/P = 15). After 4 h, the culture medium was replaced with fresh medium containing 5-flucytosine (5-FC) at various concentrations (0−160 mg/mL). After 72 h of incubation, MTT solution was added for MTT assays.

For direct observation of cell viability, HepG2 cells treated with 5-FC after transfection were stained by the FDA-PI method. HepG2 cells were seeded on 24-well plates (5×10^4 cells/well) and incubated for 24 h. Then, the culture medium was replaced with fresh medium containing the complexes (suicide gene, 1.0 μg/well, N/P = 15). After 4 h, the culture medium was replaced with fresh medium containing 40 μg/mL 5-FC. After 3 days, the treated cells were stained with 8 μL of PI (2 mg/mL in D-mannitol) and 10 μL of FDA (5 mg/mL in D-mannitol) in the dark and photographed with a fluorescence microscope (Leica DMI3000B).

2.11. In Vivo Antitumor Activity. Female balb/c-nu mice weighing 18−20 g (6−8 weeks old) were used in the antitumor activity test. HepG2 cells (2×10^6 in 100 μL of PBS) were injected subcutaneously into the middle of the right flank of the nude mice. When tumors grew to an average diameter of 5 mm, the nude mice were randomly divided into four groups. Different injections were carried out via intratumoral injection every 3 days for a total of 6 times. Details are listed as follows: Group 1, blank control (no treatment); Group 2, 25 μg of pure pCMV-CD (50 μL); Group 3, CNC-SS-PD3/pCMV-CD complexes containing 25 μg of pCMV-CD (50 μL, N/P ratio = 15); and Group 4, CNC-PD/pCMV-CD complexes containing 25 μg of pCMV-CD (50 μL, N/P ratio = 15). After 2 days, 5-FC was administered intraperitoneally at 250 mg/kg/day for 16 consecutive days with a the 5-FC concentration of 100 μg/mL.[31] Eighteen days after the first injection, all of the mice were sacrificed. The tumors obtained were dissected, photographed, and weighed.

Immunohistochemical analysis was processed as described earlier.[38] Cytosine deaminase protein expression was analyzed by rabbit polyclonal anti-cytosine deaminase antibody (RS-2950R, Shanghai

DOI: 10.1021/acsami.5b02432
ACS Appl. Mater. Interfaces 2015, 7, 8942−8951

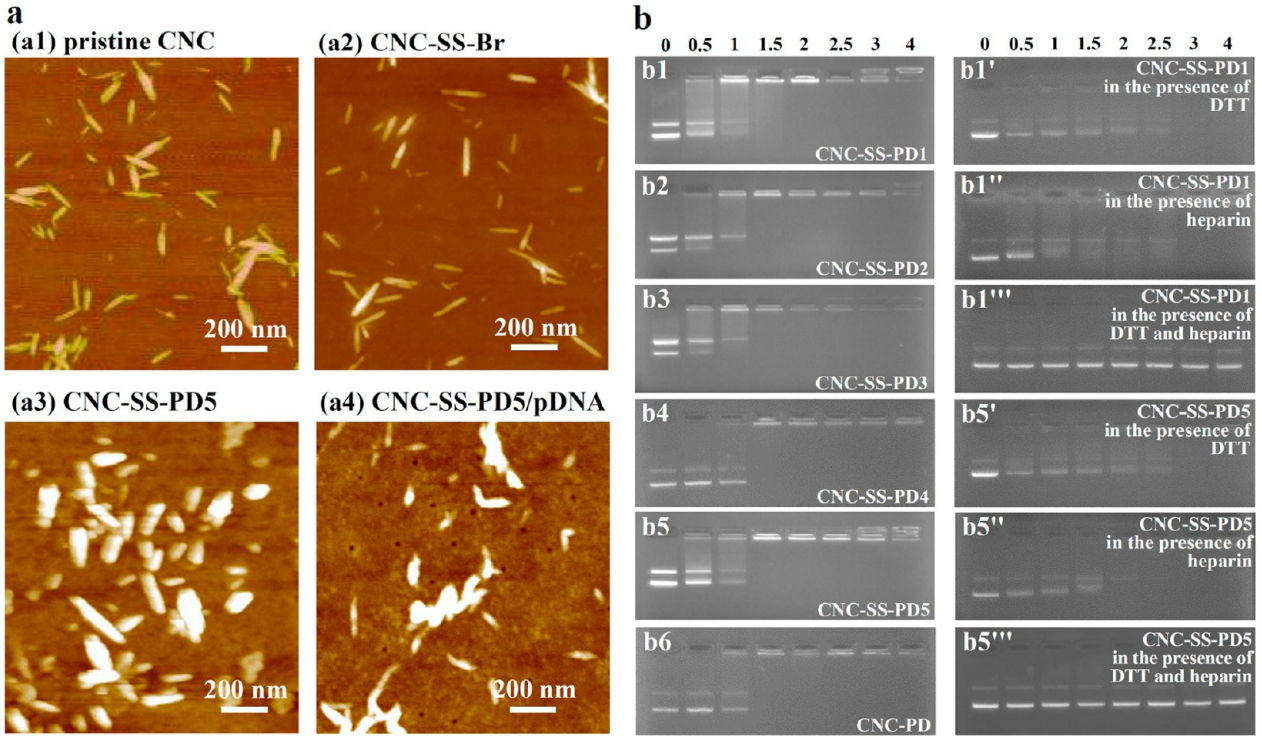

Figure 2. (a) AFM images of pristine CNC, CNC-SS-Br, CNC-SS-PD5, and CNC-SS-PD5/pDNA (N/P ratio = 5) and (b) electrophoretic mobility of pDNA in the complexes of CNC-based vectors.

Ruiqi Biological Technology, China). A cytosine deaminase-positive response was shown by a reddish-brown precipitate in the cytoplasm.

2.12. Statistical Analysis. Each experiment was performed at least three times, and data are shown as means ± standard deviation. Statistical significance ($p < 0.05$) was assessed by Student's t test.[4]

3. RESULTS AND DISCUSSION

3.1. Preparation and Characterization of CNCs with Biocleavable PDMAEMA Side Chains (CNC-SS-PDs). CNCs were prepared from the hydrolysis of cotton wool.[18] Cotton wool is composed of amorphous and crystalline sections. The numerous hydroxyl groups on CNC surfaces could be easily reacted with cystamine, giving rise to disulfide bond-containing CNCs (CNC-SS-NH_2). Then, the $-NH_2$ groups of CNC-SS-NH_2 were reacted with BIBA to give rise to bromoisobutylryl-terminated CNCs (CNC-SS-Br) for subsequent ATRP. Well-defined CNC-SS-PDs with different lengths of PDMAEMA side chains were synthesized via ATRP by controlling the reaction time. With the use of 50 mg of CNC-SS-Br, the yields (or the PDMAEMA percentages) of the resulting CNC-SS-PD products from ATRP times of 2, 5, 10, 20, and 30 min were approximately 88.1 (43.2%), 137.4 (63.6%), 203.6 (75.4%), 249.7 (79.9%), and 270.3 mg (81.5%), respectively. The yield (or PDMAEMA percentage) of the control CNC-PD without disulfide bonds was approximately 212.1 mg (or 76.4) from 10 min of ATRP.

The disulfide bonds between PDMAEMA chains and CNCs can make CNC-SS-PDs ruptur under reducing conditions. Thus, CNC-SS-PDs were treated with DL-dithiothreitol (DTT, 10 mM) for 24 h to detach the PDMAEMA side chains. The control CNC-PD was treated with 64 wt % of sulfuric acid for 3 h at 45 °C to cleave PDMAEMA. After centrifugation, the supernatant containing PDMAEMA was used for GPC assay. Table 1 summarizes the GPC results of CNC-SS-PD1 (2 min of ATRP), CNC-SS-PD2 (5 min of ATRP), CNC-SS-PD3 (10 min of ATRP), CNC-SS-PD4 (20 min of ATRP), and CNC-SS-PD5 (30 min of ATRP). The number-average molecular weight (M_n) values of PDMAEMA side chains of CNC-SS-PDs increased from 5.1×10^3 to 8.0×10^3 g/mol with increasing reaction time from 2 to 30 min. The polydispersity index of PDMEAMA was around 1.2−1.3. The M_n of PDMAEMA side chains of CNC-PD (10 min of ATRP) was 6.2×10^3 g/mol, which is similar to that of CNC-SS-PD3 (6.6×10^3 g/mol). The results indicate that the functionalization of CNCs is well-controlled by ATRP of PDMAEMA.

The chemical compositions of CNC-SS-PDs were characterized by XPS (Supporting Information, Figure S1) and FTIR (Supporting Informatino, Figure S2) spectra. The presence of the characteristic peaks confirmed the successful preparation of CNC-SS-PDs. The morphologies of CNCs, CNC-SS-Br, and CNC-SS-PD5 revealed by AFM are shown in Figure 2(a). In comparison with CNC-SS-Br, CNC-SS-PD5 still exhibited needle-like shapes. The enlarged diameter indicated that inner CNC species of CNC-SS-PD were coated by dense PDMAEMA grafts. These results demonstrate that CNCs can be easily modified by ATRP.

3.2. Characterization of CNC-SS-PD/pDNA Complexes. The capability to bind and compact pDNA is necessary for gene vectors. The condensation abilities of CNC-SS-PDs were characterized by agarose gel electrophoresis, particle size, ζ-potential, and AFM imaging. The CNC-SS-PD/pDNA complexes were first assessed by their electrophoretic mobility at different N/P ratios. Figure 2(b) illustrates the gel retardation results of CNC-SS-PD/pDNA complexes. With an N/P ratio of 2, all CNC-SS-PDs and CNC-PD can completely compact pDNA. Gene condensation ability of CNC-SS-PD is comparable to that of the control PDMAEMA

DOI: 10.1021/acsami.5b02432
ACS Appl. Mater. Interfaces 2015, 7, 8942−8951

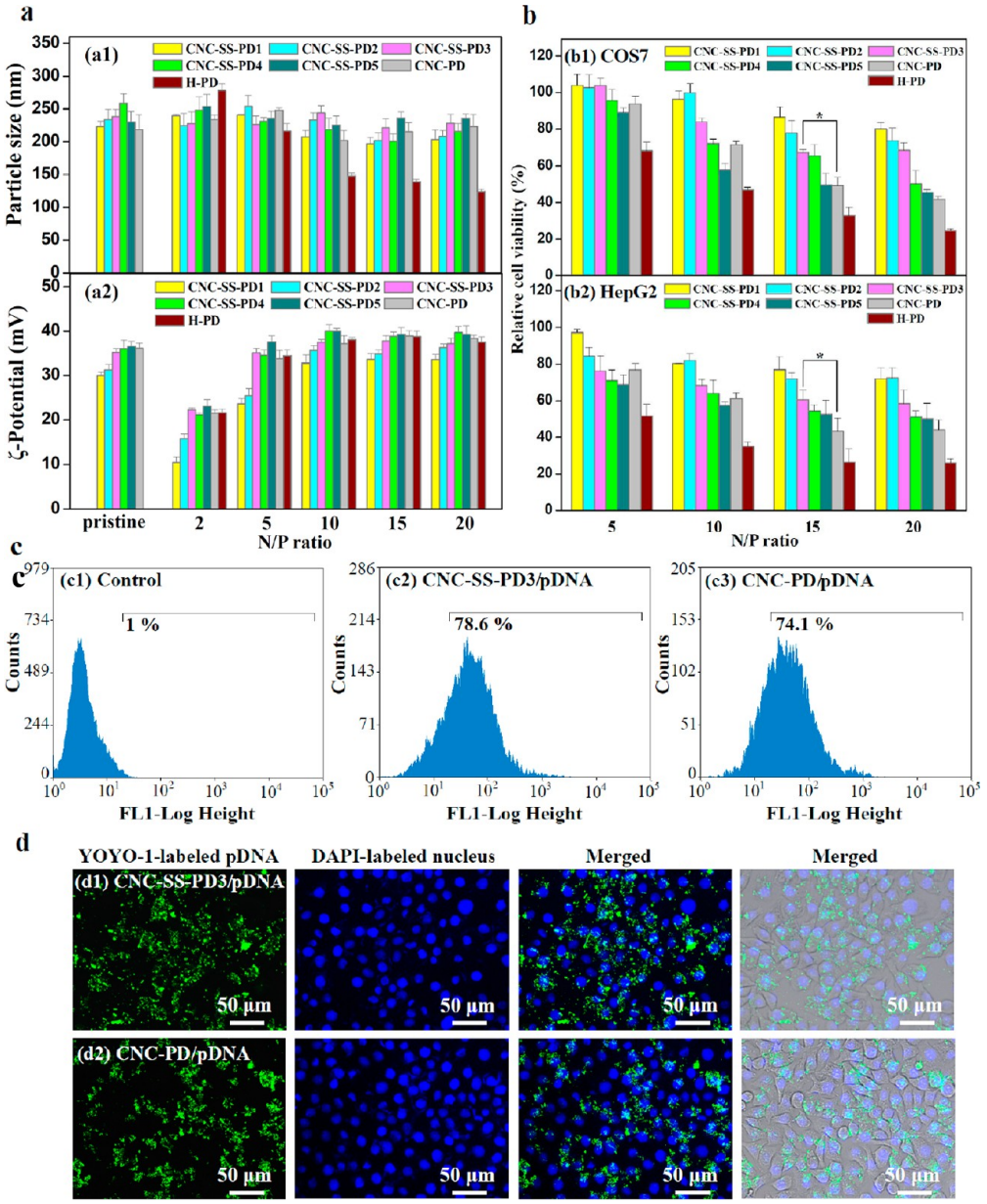

Figure 3. (a) Particle size and ζ-potential of CNC-SS-PD/pDNA, and CNC-PD/pDNA and H-PD/pDNA complexes compared to those of pristine CNC-SS-PDs and CNC-PD. (b) Cell viability of complexes in COS7 and HepG2 cells (mean ± SD, $n = 6$, $^*p < 0.05$). (c,d) Cellular internalization of (c) CNC-SS-PD3/pDNA and (d) CNC-PD/pDNA complexes at an N/P ratio of 15 in HepG2 cells (c: flow cytometry analysis plots; d: fluorescent images in which pDNA and the nucleus are shown in green and blue, respectively).

homopolymer (H-PD, $M_n \sim 2.7 \times 10^4$ g/mol) reported earlier.[10]

It is well-known that disulfide bonds can be cleaved with reducing reagents in cells, such as glutathione (GSH).[25,26] Thus, in intracellular reducible conditions, disulfide bonds between PDMAEMA chains and CNCs can be broken, promoting pDNA release from complexes. The pDNA release from CNC-SS-PD/pDNA complexes was assessed in the presence or absence of DTT, where a competitor anionic sulfated sugar, anionic heparin, was used as the model counter polyanion.[27,28,35] As shown in Figure 2(b1′,b5′), after incubation in the presence of DTT at 37 °C for 15 min, pDNA was released from the complexes of CNC-SS-PD1 and CNC-SS-PD5 up to an N/P ratio of 3. After incubation with heparin in the absence of DTT for 15 min, the CNC-SS-PD1 and CNC-SS-PD5 formulations also promoted pDNA release from their complexes (Figure 2(b1″,b5″)). Furthermore, CNC-SS-PD1 and CNC-SS-PD5 were incubated in the presence of DTT and heparin at 37 °C. After 15 min, within the test range of N/P ratios, all plasmids were clearly released (Figure 2(b1‴,b5‴)). These results indicate that under the reducible condition the detachment of PDMAEMA brushes from the CNCs could cause instability of the complexes. Such unstable complexes could be decomposed easily via interexchange with counter polyanions to promote pDNA escape from complexes. Various negatively charged cellular components exist in cells, including sulfated sugars and mRNA.[27,35] These components could act as anionic competitors to promote pDNA release. The biocleavable characteristics of CNC-SS-PDs may significantly induce pDNA release in cells and benefit the resultant gene expression.

DOI: 10.1021/acsami.5b02432
ACS Appl. Mater. Interfaces 2015, 7, 8942−8951

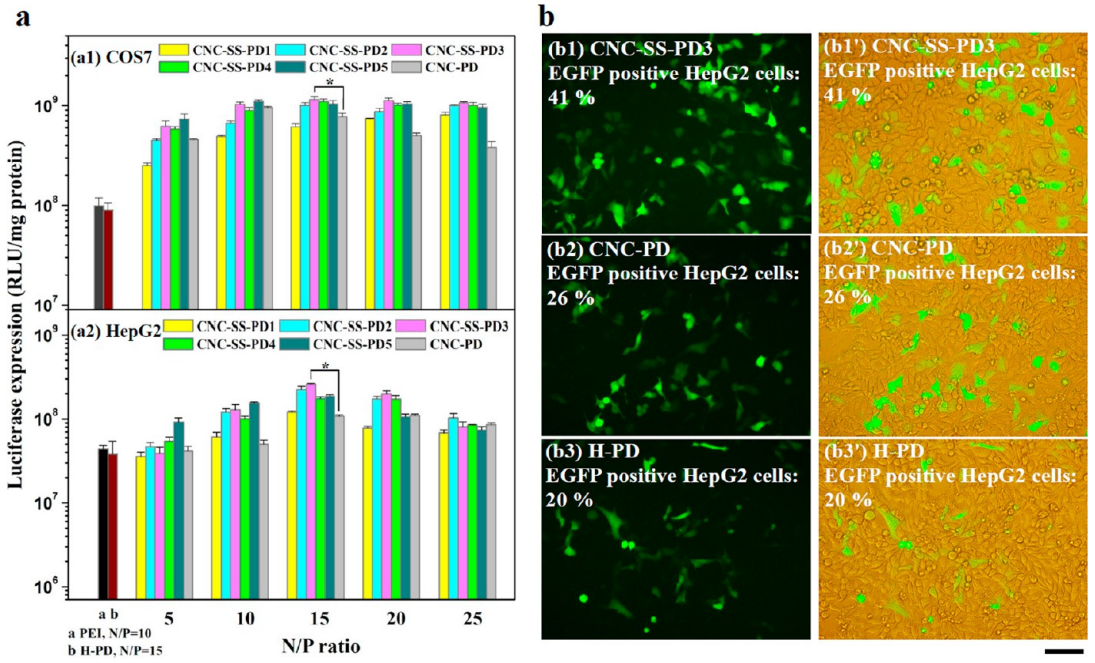

Figure 4. (a) In vitro luciferase gene expression mediated by CNC-SS-PDs and CNC-PD in comparison with those mediated by H-PD and PEI in COS7 and HepG2 cells (mean ± SD, $n = 3$, $^*p < 0.05$), and (b) representative images of pEGFP expression mediated by CNC-SS-PD3, CNC-PD, and H-PD at an N/P ratio of 15 in HepG2 cells (scale bar: 50 μm).

The particle sizes and ζ-potentials of CNC-SS-PD/pDNA complexes at different N/P ratios are illustrated in Figure 3(a). After the formation of complexes, no significant changes were observed in particle sizes in the range of 200−250 nm. Complexes in this size range can readily undergo endocytosis. The sizes of nanoparticles for ready cellular uptake can range from nano- to micrometers by endocytosis.[14,39] In this work, particles with diameters <250 nm may be internalized rapidly. Figure 2(a4) exhibits AFM images of CNC-SS-PD5/pDNA complexes at an N/P ratio of 5. In comparison with CNC-SS-PD5 (Figure 2(a3)), the complexes still displayed needle-like shapes, and the diameter was largely decreased. PDMAEMA brushes underwent shrinkage after complexation with pDNA, leading to the decrease in diameter. These results indicate that pDNA can be effectively compacted by CNC-SS-PD and that the needle-like morphologies of CNCs remain unchanged.

The positively charged surface can allow electrostatic interaction with a negatively charged cell membrane to facilitate cellular uptake.[40] Zeta-potential is an indicator of complex surface charges. As shown in Figure 3(a2), the surface charges of the complexes remained positive from N/P ratios of 2−20. At N/P ratios above 10, CNC-SS-PD/pDNA complexes contained excess cationic CNC-SS-PD vectors, which made the ζ-potentials approach those of the pristine CNC-SS-PDs. The positive surface charge would contribute good affinity to the anionic cell membrane.

3.3. Cell Viability Assay. A good vector should possess high transfection efficiency with reasonable cytotoxicity. CNCs could penetrate cells with no indication of cytotoxicity.[19] The cell viability of CNC-SS-PD/pDNA complexes was evaluated in COS7 and HepG2 cells at various N/P ratios by MTT assay (Figure 3(b)). Here, the cytotoxicity of the control CNC-PD and H-PD was examined for comparison. As the N/P ratio increased, the cell viability of all CNC-SS-PD/pDNA complexes decreased. The increased cell cytotoxicity was ascribed to the fact that, at high N/P ratios, excess free CNC-SS-PDs exist in addition to the compact complexes. At the same N/P ratio, the cell viability of CNC-SS-PDs seemed to be associated with the length of the PDMAEMA chains. The longer chains exhibited higher toxicity. Because of the increased length of PDMAEMA chains from CNC-SS-PD1 to CNC-SS-PD5, their cytotoxicity exhibited an increasing trend. This is consistent with the fact that high molecular weight polycations exhibit higher cytotoxicity.[41] These results show that the length of the PDMAEMA chains can be adjusted to control the cytotoxicity of CNC-SS-PDs.

As shown in Table 1, CNC-SS-PD3 and CNC-PD possess similar lengths of PDMAEMA chains. However, at most N/P ratios, CNC-SS-PD3 shows much higher cell viability than CNC-PD. As illustrated in Table 1 and Figure 2(b), disulfide bonds in CNC-SS-PD could be triggered by GSH.[42] The PDMAEMA side chains of CNC-SS-PDs could be rapidly detached from CNC nanocrystals after cellular internalization. Such detachment of low molecular weight PDMAEMA side chains may contribute to the higher cellular activity of CNC-SS-PD3. In addition, CNC-PD exhibits significantly lower cytotoxicity than H-PD, probably because of the introduction of nontoxic CNCs.

3.4. Cellular Internalization. Cellular uptake of CNC-based complexes was investigated by flow cytometry in HepG2 cells, where pDNA was labeled with YOYO-1 fluorescence dye. The efficiency of cellular uptake was determined by assaying the intensity of fluorescence that was emitted by the positive cells. As illustrated in Figure 3(c), internalization rates of CNC-SS-PD3/pDNA complexes and CNC-PD/pDNA complexes were 78.6% and 74.1%, respectively. The similar internalization rates show that introduction of the disulfide bond has no effect on the process of cellular uptake. Fluorescent images of cellular uptake are shown in Figure 3(d). The polycation/pDNA complexes are shown in green fluorescence, and nuclei stained with DAPI are shown in blue fluorescence. There are no significant differences in the green fluorescent signal between

DOI: 10.1021/acsami.5b02432
ACS Appl. Mater. Interfaces 2015, 7, 8942−8951

the cells treated with CNC-SS-PD3/pDNA and CNC-PD/pDNA.

3.5. In Vitro Gene Transfection Assay. The transfection performance of CNC-SS-PD/pDNA complexes was first evaluated with pRL-CMV in COS7 and HepG2 cells. PEI (25 kDa, a common commercial transfection reagent) and H-PD were used as controls. Figure 4(a) shows the transfection efficiency of complexes at different N/P ratios compared to those of PEI (at its optimal N/P ratio of 10[43]) and H-PD (N/P ratio of 15[32,43]). The transfection efficiency increased at low N/P ratios first and then remained constant or declined slightly with a further increase in the N/P ratio. At low N/P ratios, polycations cannot effectively condense pDNA into nanocomplexes. The resulting loose complexes cannot be easily internalized by cells. At an N/P ratio of ~15, optimal transfection efficiencies were obtained for most complexes. However, at higher N/P ratios, free polycations that did not bind with pDNA existed in the transfection formulation, leading to increasing cytotoxicity (Figure 3(b)). The increased cytotoxicity then resulted in decreased transfection efficiency.

CNC-SS-PD5 exhibited a higher transfection efficiency than that of CNC-SS-PD1 at most N/P ratios (particularly at low N/P ratios). This phenomenon indicates that the transfection efficiencies of CNC-SS-PDs depend on the length of the PDMAEMA chains. It was well-known that polycations with high molecular weight possess better transfection performance.[32,43] Long PDMAEMA chains can enhance the binding ability with negatively charged pDNA, and the resulting tight and stable complex benefits with better transfection efficiency. At most N/P ratios in COS7 and HepG2 cells, CNC-SS-PD3 demonstrated much higher transfection efficiencies than CNC-PD even though they possess similar internalization rates (Figure 3(c)). As mentioned earlier, the molecular weights of PDMAEMA chains were very similar between CNC-SS-PD3 and CNC-PD. These results indicate that the transfection efficiency can indeed be improved with the introduction of disulfide bonds because they are responsive to reducing reagents, such as GSH. Intracellular reducible conditions could break the disulfide bridge linkages and make PDMAEMA detach from CNCs. As shown in Figure 2(b), the reducible conditions could promote pDNA escape from complexes, which can benefit the resultant gene expression.[28,29,32] In addition, all CNC-SS-PDs exhibited substantially higher transfection efficiencies than those mediated by PEI and H-PD. This may be due to the good biocompatibility and appropriate aspect ratio of the CNC substrate. Rodlike particles are internalized faster than spherical particles.[14] Our earlier work indicated that the dimensions and shape of nanoparticles have a large influence on gene transfection and that the rodlike NPs exhibited better gene transfection performance.[4]

The outstanding transfection performance of biocleavable vectors was observed intuitively with fluorescence microscopy in HepG2 cells. Representative images of pEGFP gene expression are shown in Figure 4(b). The percentages of the EGFP-positive cells (determined by flow cytometry[20]) for CNC-SS-PD3, CNC-PD, and H-PD were approximately 41%, 26%, and 20%, respectively. The cells that were treated with CNC-SS-PD3/pEGFP complexes exhibited more intense green fluorescence than those treated with the CNC-PD/pEGFP and H-PD/pEGFP complexes. These results are in accordance with that of luciferase expression (Figure 4(a)).

3.6. In Vitro Antitumor Effects with a CD/5-FC Suicide Gene System. The antitumor effect of CNC-SS-PD3 and CNC-PD was assessed at different 5-FC concentrations in HepG2 cells. Hepatoma is a common cancer. HepG2 is a perpetual cell line consisting of human liver carcinoma cells and has been widely used for scientific research.[4,10,23] CD/5-FC is one widely investigated suicide gene/prodrug system in treating tumors.[31] 5-FC could be transformed to highly cytotoxic 5-fluorouracil (5-FU) under the action of CD. which can then spread to surrounding cells and kill them.[44,45] The effective introduction of the CD gene in cancerous cells is an important step. As shown in Figure 5(a), at an N/P ratio of 15, the

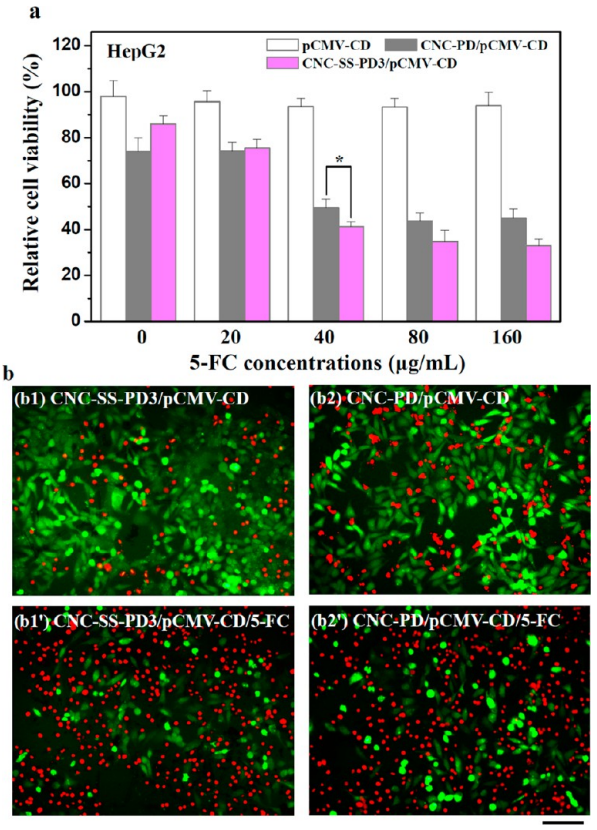

Figure 5. (a) Cell viability of the HepG2 cells treated with various concentrations of 5-FC after transfection mediated by pCMV-CD, CNC-SS-PD3/pCMV-CD (N/P ratio = 15), and CNC-PD/pCMV-CD (N/P ratio = 15) complexes (mean ± SD, $n = 6$, $*p < 0.05$), and (b) FDA-PI staining mediated by CNC-SS-PD3/pCMV-CD and CNC-PD/pCMV-CD at an N/P ratio of 15 (b1, b2: absence of 5-FC; b1′, b2′: presence of 5-FC (40 μg/mL); live cells: green; dead cells: red; scale bar: 50 μm).

viability of the HepG2 cells declined with the increasing concentration of 5-FC. When the concentration of 5-FC reached 40 μg/mL or higher, the viability of HepG2 cells that were treated with the CNC-SS-PD3/pCMV-CD complexes was <42%, lower than those treated with the CNC-PD/pCMV-CD complexes. Such a result was consistent with their corresponding transfection efficiencies (Figure 4(a)). CNC-SS-PD3 demonstrated the higher transfection efficiency, allowing for the CD gene to be expressed more efficiently. Thus, good antitumor ability could be readily achieved with biocleavable CNC-SS-PD vectors.

Cell viability was also observed directly by FDA-PI staining. FDA, a nonfluorescent molecule, can hydrolyze by nonspecific esterases in viable cells to emit green fluorescence in the cytoplasm. The nucleic acid binding dye, PI, can readily enter

DOI: 10.1021/acsami.5b02432
ACS Appl. Mater. Interfaces 2015, 7, 8942−8951

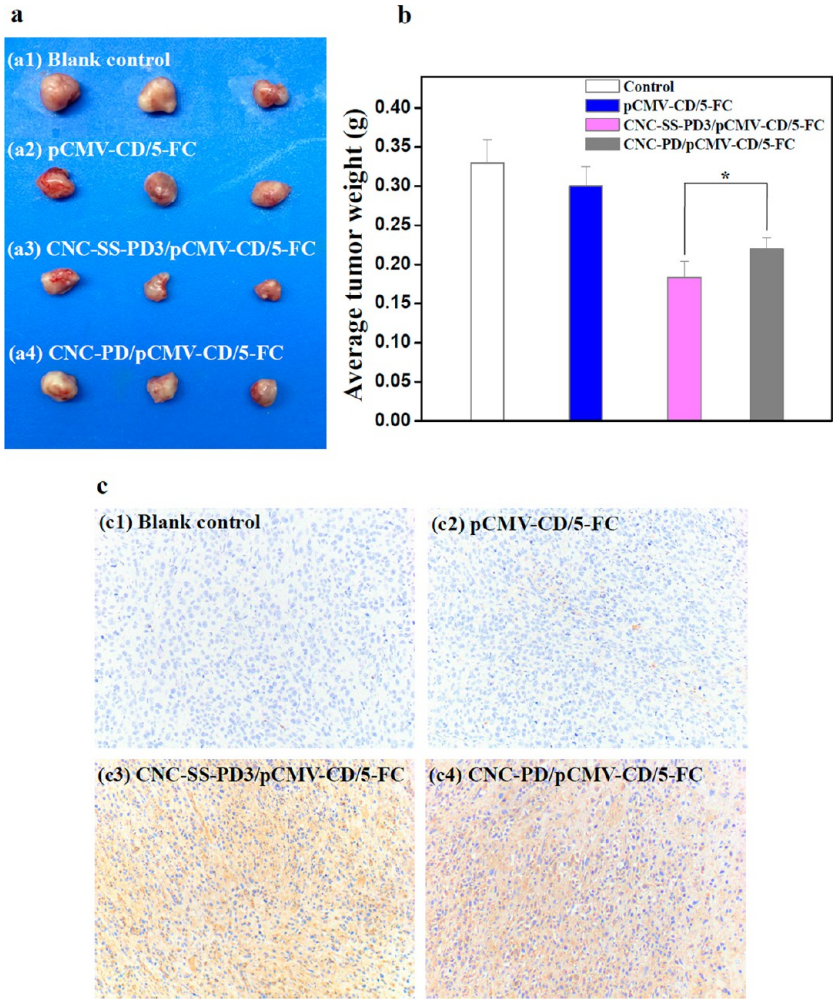

Figure 6. Antitumoral therapeutic effects in female balb/c nude mice after intratumoral injection of pCMV-CD/5-FC, CNC-SS-PD3/pCMV-CD/5-FC, and CNC-PD/pCMV-CD/5-FC: (a) images and (b) weights of tumors after the different treatments for 18 days (mean ± SD, $n = 3$, $^*p < 0.05$), and (c) immunohistochemical staining assay of tumor tissues performed using specific antibodies against cytosine deaminase.

apoptotic/dead cells and emit red fluorescence. Thus, FDA-PI staining can differentiate viable cells (in green) and dead cells (in red).[33] As shown in Figure 5(b), it was distinctly observed that HepG2 cells were inhibited or killed when treated with the CNC-SS-PD3/pCMV-CD and CNC-PD/pCMV-CD complexes in the presence of 5-FC. The HepG2 cells that were treated with CNC-SS-PD3/pCMV-CD complexes demonstrated more red fluorescent cells, which was consistent with the in vitro 5-FC sensitivity assay (Figure 5(a)).

3.7. In Vivo Antitumor Activity. On the basis of the in vitro antitumor assay, CNC-SS-PD3 and CNC-PD were further used to deliver pCMV-CD in vivo to investigate the suppression and regression of tumor growth. The photos and weights of tumors are shown in Figure 6(a,b). Compared to mice treated with pure pCMV-CD in the presence of 5-FC, the tumors of the mice treated with the CNC-SS-PD3/pCMV-CD and CNC-PD/pCMV-CD complexes were much smaller. Furthermore, the CNC-SS-PD3/pCMV-CD group presented the lowest tumor weight, nearly half that of the tumors treated with pCMV-CD (Figure 6(b)). The results were consistent with the in vitro CD/5-FC cytotoxicity assay (Figure 5(a)), indicating that the CNC-based carriers could suppress and regress the tumor growth in vivo. The introduction of disulfide bonds also improved the in vivo antitumor efficacy.

Immunohistochemical analysis of the dissected tumor tissues was also performed to confirm the in vivo expression of the CD gene of CNC-based carriers. In comparison with the control (Figure 6(c1)) and pCMV-CD (Figure 6(c2)) groups, large reddish-brown area segmentations were observed clearly in the CNC-SS-PD3/pCMV-CD (Figure 6(c3)) and CNC-PD/pCMV-CD (Figure 6(c4)) groups. This phenomena indicated that cytosine deaminase was clearly expressed in tumor sections of mice treated with CNC-SS-PD3/pCMV-CD/5-FC and CNC-PD/pCMV-CD/5-FC complexes. These results clearly demonstrate that CNC-based polycation carriers can efficiently deliver pCMV-CD into tumor tissues and subsequently inhibit tumor growth in mice.

4. CONCLUSION

Disulfide bond-linked PDMAEMA side chains were successfully grafted from needle-like CNCs via surface-initiated ATRP for effective gene therapy. The resultant CNC-SS-PDs were characterized by XPS, FTIR, and AFM. Under reducing conditions, PDMAEMA side chains could readily be cleaved from CNCs, and CNC-SS-PD/pDNA complexes disintegrated, promoting the release of pDNA. Compared to PEI (25 kDa), H-PD, and CNC-PD, the bioreducible CNC-SS-PDs showed higher transfection efficiencies and lower cytotoxicities. CNC-

DOI: 10.1021/acsami.5b02432
ACS Appl. Mater. Interfaces 2015, 7, 8942−8951

SS-PD also demonstrated good activity in suppressing the growth of cancer cells and tumors. Therefore, properly grafting redox-responsive polycation chains from CNCs is a useful method to make novel smart gene/drug delivery systems.

■ ASSOCIATED CONTENT

Supporting Information

XPS and FTIR spectra details. This material is available free of charge via the Internet at http://pubs.acs.org.

■ AUTHOR INFORMATION

Corresponding Authors

*E-mail: xufj@mail.buct.edu.cn.
*E-mail: majie1965@163.com.

Author Contributions

△These authors contributed equally to this work.

Notes

The authors declare no competing financial interest.

■ ACKNOWLEDGMENTS

This work was partially supported by National Natural Science Foundation of China (Grants 51473014, 51221002, and 51325304), National High Technology Development Program of China (863 Program 2014AA020519), Beijing Natural Science Foundation (Project No. 7151002), Beijing Nova Program (Z131107000413066), and Collaborative Innovation Center for Cardiovascular Disorders, Beijing Anzhen Hospital affiliated with Capital Medical University.

■ REFERENCES

(1) Anderson, W. F. Human Gene Therapy. *Nature* **1998**, *392*, 25−30.
(2) Guo, X.; Huang, L. Recent Advances in Nonviral Vectors for Gene Delivery. *Acc. Chem. Res.* **2012**, *45*, 971−979.
(3) Duarte, S.; Carle, G.; Faneca, H.; de Lima, M. C.; Pierrefite-Carle, V. Suicide Gene Therapy in Cancer: Where Do We Stand Now? *Cancer Lett.* **2012**, *324*, 160−170.
(4) Lin, X.; Zhao, N.; Yan, P.; Hu, H.; Xu, F. J. The Shape and Size Effects of Polycation Functionalized Silica Nanoparticles on Gene Transfection. *Acta Biomater.* **2015**, *11*, 381−392.
(5) Yudovin-Farber, I.; Domb, A. J. Cationic Polysaccharides for Gene Delivery. *Mater. Sci. Eng., C* **2007**, *27*, 595−598.
(6) Verma, I. M.; Somia, N. Gene Therapy - Promises, Problems and Prospects. *Nature* **1997**, *389*, 239−242.
(7) Roesler, S.; Koch, F. P.; Schmehl, T.; Weissmann, N.; Seeger, W.; Gessler, T.; Kissel, T. Amphiphilic, Low Molecular Weight Poly(ethylene imine) Derivatives with Enhanced Stability for Efficient Pulmonary Gene Delivery. *J. Gene Med.* **2011**, *13*, 123−133.
(8) Tian, H.; Lin, L.; Chen, J.; Chen, X.; Park, T. G.; Maruyama, A. RGD Targeting Hyaluronic Acid Coating System for PEI-PBLG Polycation Gene Carriers. *J. Controlled Release* **2011**, *155*, 47−53.
(9) Saranya, N.; Moorthi, A.; Saravanan, S.; Devi, M. P.; Selvamurugan, N. Chitosan and Its Derivatives for Gene Delivery. *Int. J. Biol. Macromol.* **2011**, *48*, 234−238.
(10) Hu, H.; Xiu, K. M.; Xu, S. L.; Yang, W. T.; Xu, F. J. Functionalized Layered Double Hydroxide Nanoparticles Conjugated with Disulfide-Linked Polycation Brushes for Advanced Gene Delivery. *Bioconjugate Chem.* **2013**, *24*, 968−978.
(11) Liu, J.; Xu, Y.; Yang, Q.; Li, C.; Hennink, W. E.; Zhuo, R.; Jiang, X. Reduction Biodegradable Brushed PDMAEMA Derivatives Synthesized by Atom Transfer Radical Polymerization and Click Chemistry for Gene Delivery. *Acta Biomater.* **2013**, *9*, 7758−7766.
(12) Zhang, X.; Ma, G. H.; Su, Z. G.; Benkirane-Jessel, N. Novel poly(L-lysine) Particles for Gene Delivery. *J. Controlled Release* **2011**, *152*, e182−e184.
(13) Singh, R.; Lillard, J. W., Jr. Nanoparticle-Based Targeted Drug Delivery. *Exp. Mol. Pathol.* **2009**, *86*, 215−223.
(14) Gratton, S. E.; Ropp, P. A.; Pohlhaus, P. D.; Luft, J. C.; Madden, V. J.; Napier, M. E.; DeSimone, J. M. The Effect of Particle Design on Cellular Internalization Pathways. *Proc. Natl. Acad. Sci. U.S.A.* **2008**, *105*, 11613−11618.
(15) Liu, M.; Chen, B.; Xue, Y.; Huang, J.; Zhang, L.; Huang, S.; Li, Q.; Zhang, Z. Polyamidoamine-Grafted Multiwalled Carbon Nanotubes for Gene Delivery: Synthesis, Transfection and Intracellular Trafficking. *Bioconjugate Chem.* **2011**, *22*, 2237−2243.
(16) Clift, M. J.; Foster, E. J.; Vanhecke, D.; Studer, D.; Wick, P.; Gehr, P.; Rothen-Rutishauser, B.; Weder, C. Investigating the Interaction of Cellulose Nanofibers Derived from Cotton with a Sophisticated 3D Human Lung Cell Coculture. *Biomacromolecules* **2011**, *12*, 3666−3673.
(17) de Souza Lima, M. M.; Borsali, R. Rodlike Cellulose Microcrystals: Structure, Properties, and Applications. *Macromol. Rapid Commun.* **2004**, *25*, 771−787.
(18) Habibi, Y.; Lucia, L. A.; Rojas, O. J. Cellulose Nanocrystals: Chemistry, Self-assembly, and Applications. *Chem. Rev.* **2010**, *110*, 3479−3500.
(19) Mahmoud, K. A.; Mena, J. A.; Male, K. B.; Hrapovic, S.; Kamen, A.; Luong, J. H. Effect of Surface Charge on the Cellular Uptake and Cytotoxicity of Fluorescent Labeled Cellulose Nanocrystals. *ACS Appl. Mater. Interfaces* **2010**, *2*, 2924−2932.
(20) Morandi, G.; Heath, L.; Thielemans, W. Cellulose Nanocrystals Grafted with Polystyrene Chains Through Surface-Initiated Atom Transfer Radical Polymerization (SI-ATRP). *Langmuir* **2009**, *25*, 8280−8286.
(21) Moon, R. J.; Martini, A.; Nairn, J.; Simonsen, J.; Youngblood, J. Cellulose Nanomaterials Review: Structure, Properties and Nanocomposites. *Chem. Soc. Rev.* **2011**, *40*, 3941−3994.
(22) Terech, P.; Chazeau, L.; Cavaille, J. Y. A Small-Angle Scattering Study of Cellulose Whiskers in Aqueous Suspensions. *Macromolecules* **1999**, *32*, 1872−1875.
(23) Xu, F. J.; Yang, W. T. Polymer Vectors via Controlled/Living Radical Polymerization for Gene Delivery. *Prog. Polym. Sci.* **2011**, *36*, 1099−1131.
(24) Meng, F.; Hennink, W. E.; Zhong, Z. Reduction-Sensitive Polymers and Bioconjugates for Biomedical Applications. *Biomaterials* **2009**, *30*, 2180−2198.
(25) Saito, G.; Swanson, J. A.; Lee, K. D. Drug Delivery Strategy Utilizing Conjugation via Reversible Disulfide Linkages: Role and Site of Cellular Reducing Activities. *Adv. Drug Delivery Rev.* **2003**, *55*, 199−215.
(26) Ho, Y. C.; Liao, Z. X.; Panda, N.; Tang, D. W.; Yu, S. H.; Mi, F. L.; Sung, H. W. Self-organized Nanoparticles Prepared by Guanidine- and Disulfide-Modified Chitosan as a Gene Delivery Carrier. *J. Mater. Chem.* **2011**, *21*, 16918−16927.
(27) Kang, H. C.; Kang, H. J.; Bae, Y. H. A Reducible Polycationic Gene Vector Derived from Thiolated Low Molecular Weight Branched Polyethyleneimine Linked by 2-iminothiolane. *Biomaterials* **2011**, *32*, 1193−1203.
(28) Neu, M.; Germershaus, O.; Mao, S.; Voigt, K. H.; Behe, M.; Kissel, T. Crosslinked Nanocarriers Based upon Poly(ethylene imine) for Systemic Plasmid Delivery: *in vitro* Characterization and *in vivo* Studies in Mice. *J. Controlled Release* **2007**, *118*, 370−380.
(29) Manickam, D. S.; Oupicky, D. Multiblock Reducible Copolypeptides Containing Histidine-Rich and Nuclear Localization Sequences for Gene Delivery. *Bioconjugate Chem.* **2006**, *17*, 1395−1403.
(30) Matyjaszewski, K.; Xia, J. Atom Transfer Radical Polymerization. *Chem. Rev.* **2001**, *101*, 2921−2990.
(31) Liang, B.; He, M. L.; Chan, C. Y.; Chen, Y. C.; Li, X. P.; Li, Y.; Zheng, D.; Lin, M. C.; Kung, H. F.; Shuai, X. T.; Peng, Y. The Use of Folate-PEG-Grafted-Hybranched-PEI Nonviral Vector for the Inhibition of Glioma Growth in the Rat. *Biomaterials* **2009**, *30*, 4014−4020.
(32) Wang, Z. H.; Zhu, Y.; Chai, M. Y.; Yang, W. T.; Xu, F. J. Biocleavable Comb-Shaped Gene Carriers from Dextran Backbones

DOI: 10.1021/acsami.5b02432
ACS Appl. Mater. Interfaces 2015, 7, 8942−8951

with Bioreducible ATRP Initiation Sites. *Biomaterials* **2012**, *33*, 1873−1883.
(33) Li, Y.; Han, X. Microcystin-LR Causes Cytotoxicity Effects in Rat Testicular Sertoli Cells. *Environ. Toxicol. Pharmacol.* **2012**, *33*, 318−326.
(34) Xu, F. J.; Li, H.; Li, J.; Zhang, Z.; Kang, E. T.; Neoh, K. G. Pentablock Copolymers of Poly(ethylene glycol), Poly((2-dimethyl amino)ethyl methacrylate) and Poly(2-hydroxyethyl methacrylate) from Consecutive Atom Transfer Radical Polymerizations for Non-viral Gene Delivery. *Biomaterials* **2008**, *29*, 3023−3033.
(35) Chen, D.; Ping, Y.; Tang, G. P.; Li, J. Polyethyleneimine-Grafted Poly(*N*-3-hydroxypropyl) Aspartamide as a Biodegradable Gene Vector for Efficient Gene Transfection. *Soft Matter* **2010**, *6*, 955−964.
(36) Dai, F.; Liu, W. Enhanced Gene Transfection and Serum Stability of Polyplexes by PDMAEMA-polysulfobetaine Diblock Copolymers. *Biomaterials* **2011**, *32*, 628−638.
(37) Wang, Z. H.; Li, W. B.; Ma, J.; Tang, G. P.; Yang, W. T.; Xu, F. J. Functionalized Nonionic Dextran Backbones by Atom Transfer Radical Polymerization for Efficient Gene Delivery. *Macromolecules* **2011**, *44*, 230−239.
(38) Wang, L.; Wei, D.; Huang, S.; Peng, Z.; Le, X.; Wu, T. T.; Yao, J.; Ajani, J.; Xie, K. Transcription Factor Sp1 Expression is a Significant Predictor of Survival in Human Gastric Cancer. *Clin. Cancer Res.* **2003**, *9*, 6371−6380.
(39) Rejman, J.; Oberle, V.; Zuhorn, I. S.; Hoekstra, D. Size-Dependent Internalization of Particles via the Pathways of Clathrin- and Caveolae-Mediated Endocytosis. *Biochem. J.* **2004**, *377*, 159−169.
(40) Mastrobattista, E.; Hennink, W. E. Polymers for Gene Delivery: Charged for Success. *Nat. Mater.* **2012**, *11*, 10−12.
(41) van de Wetering, P.; Moret, E. E.; Schuurmans-Nieuwenbroek, N. M.; van Steenbergen, M. J.; Hennink, W. E. Structure-Activity Relationships of Water-Soluble Cationic Methacrylate/Methacrylamide Polymers for Nonviral Gene Delivery. *Bioconjugate Chem.* **1999**, *10*, 589−597.
(42) You, Y. Z.; Manickam, D. S.; Zhou, Q. H.; Oupicky, D. Reducible Poly(2-dimethylaminoethyl methacrylate): Synthesis, Cytotoxicity, and Gene Delivery Activity. *J. Controlled Release* **2007**, *122*, 217−225.
(43) Ping, Y.; Liu, C. D.; Tang, G. P.; Li, J. S.; Li, J.; Yang, W. T.; Xu, F. J. Functionalization of Chitosan via Atom Transfer Radical Polymerization for Gene Delivery. *Adv. Funct. Mater.* **2010**, *20*, 3106−3116.
(44) Chen, J. K.; Hu, L. J.; Wang, D.; Lamborn, K. R.; Deen, D. F. Cytosine Deaminase/5-fluorocytosine Exposure Induces Bystander and Radiosensitization Effects in Hypoxic Glioblastoma Cells *in vitro*. *Int. J. Radiat. Oncol., Biol., Phys.* **2007**, *67*, 1538−1547.
(45) Lawrence, T. S.; Rehemtulla, A.; Ng, E. Y.; Wilson, M.; Trosko, J. E.; Stetson, P. L. Preferential Cytotoxicity of Cells Transduced with Cytosine Deaminase Compared to Bystander Cells after Treatment with 5-flucytosine. *Cancer Res.* **1998**, *58*, 2588−2593.

DOI: 10.1021/acsami.5b02432
ACS Appl. Mater. Interfaces 2015, 7, 8942−8951